iScience, Volume *24*

Supplemental information

Functional organization of the maternal and paternal human 4D Nucleome

Stephen Lindsly, Wenlong Jia, Haiming Chen, Sijia Liu, Scott Ronquist, Can Chen, Xingzhao Wen, Cooper Stansbury, Gabrielle A. Dotson, Charles Ryan, Alnawaz Rehemtulla, Gilbert S. Omenn, Max Wicha, Shuai Cheng Li, Lindsey Muir, and Indika Rajapakse

Supplemental Figures

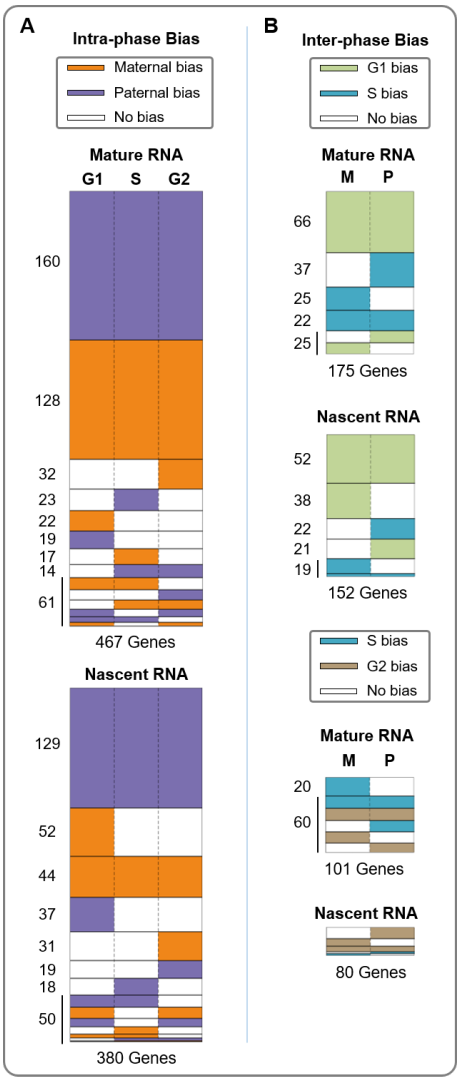

Fig. S1: Expression biases identified between alleles and cell cycle phases, related to **Figure 3**. **(A)** Differential expression between the maternal and paternal alleles for each cell cycle phase. Differentially expressed genes with a bias towards the maternal (paternal) allele in a particular cell cycle phase are shaded orange (purple). Each row represents a group of genes with a specific expression bias pattern. **(B)** Differential expression between cell cycle phases within each allele. Top shows differential expression between G1 and S phases while bottom shows differential expression between S and G2. Genes are shaded in the color of the cell cycle phase in which their expression is significantly higher. G1, S, and G2 are shaded green, blue, brown respectively. In both (A) and (B), white represents no expression bias.

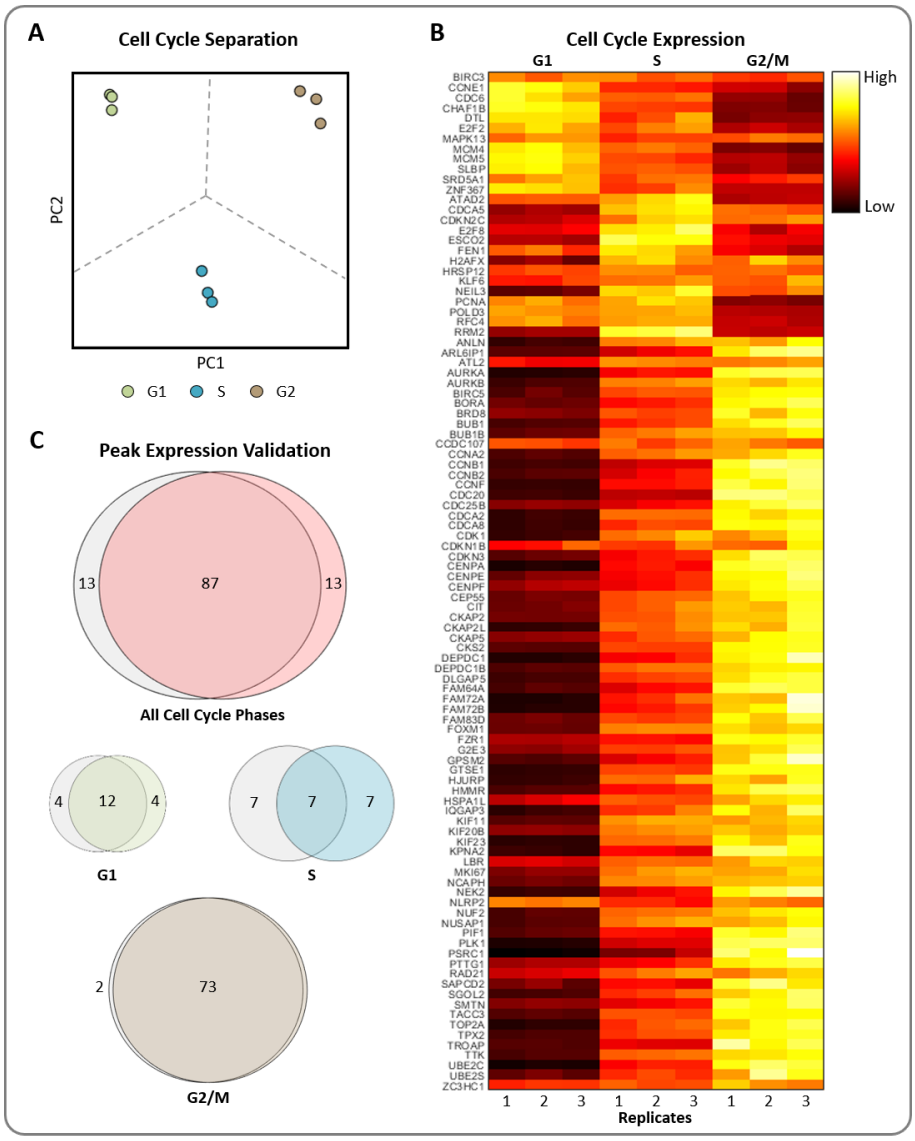

Fig. S2: Cell cycle separation of RNA-seq data, related to **STAR Methods**. **(A)** Principal component analysis (PCA) of three replicates over three time points. G1, S, and G2 are easily separated and the replicates of each cell cycle phase cluster after dimension reduction. **(B)** RNA-seq expression heatmap of the top 100 periodically expressed genes in our data from Cyclebase are row normalized and clustered by peak expression time (*80*). **(C)** Venn diagram comparison for the peak expression time of the same 100 periodically expressed genes. Red, green, blue, and brown circles represent the peak expression times for G1, S, and G2 within our data respectively, and overlap with gray indicates agreement with Cyclebase peak expression times. Over all phases, 87% of these genes match in their peak expression cell cycle phase.

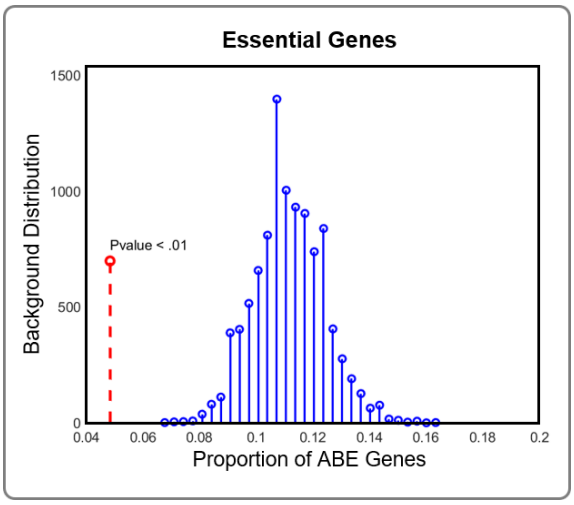

Fig. S3: Statistical significance of decreased ABE in essential genes, related to **STAR Methods**. A permutation test was performed to determine whether essential genes were less likely to have ABE versus randomly sampled allele-specific genes (**Method Details**).

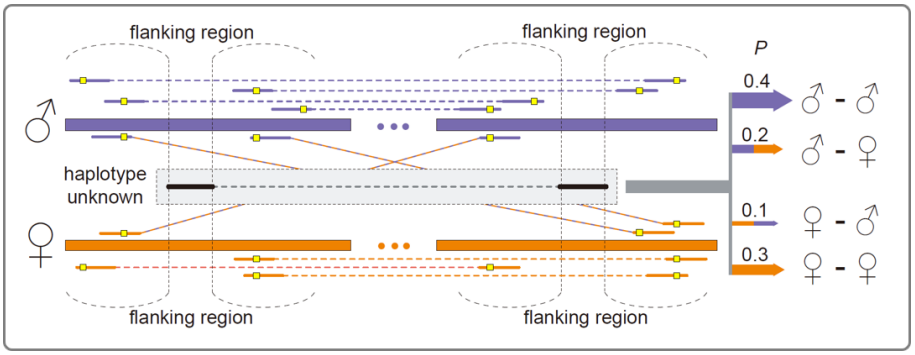

Fig. S4: Expanded diagram of HaploHiC phasing, related to **Figure 4**. Haplotype-unknown Hi-C pair is distributed to certain haplotype combination with probabilities depending on local phased contacts in flanking regions. Homologous genomic regions are linked by phased Hi-C pairs (purple for paternal, orange for maternal). Phased heterozygous loci are denoted by yellow squares.

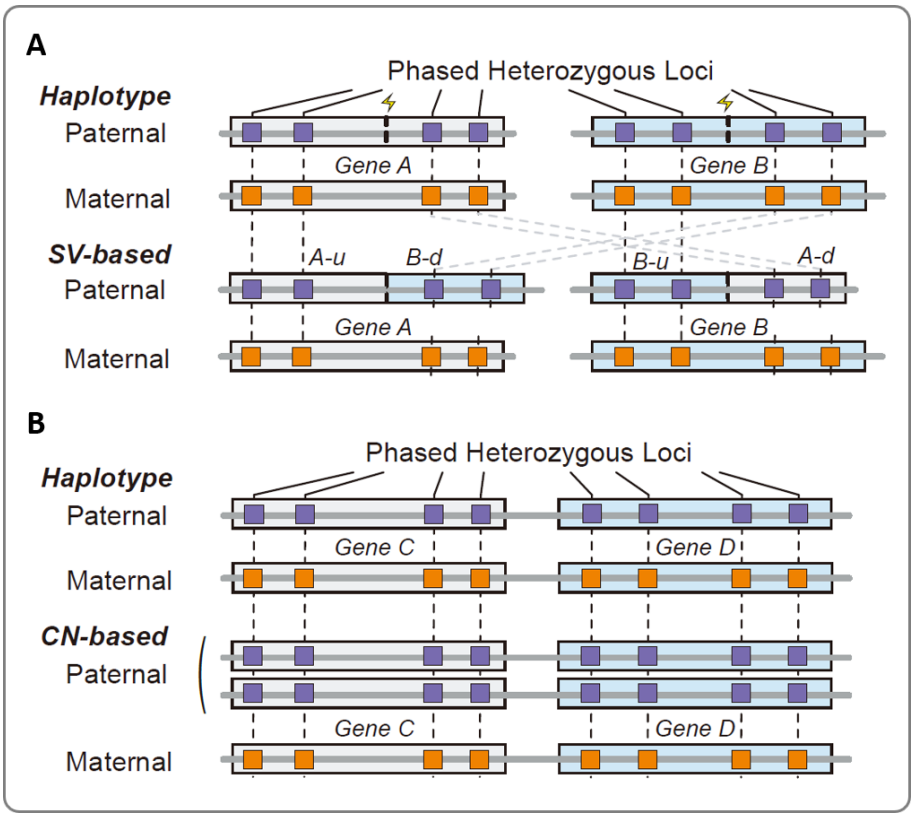

Fig. S5: Simulation of SV-based and CN-based contacts, related to **STAR Methods**. **(A)** Gene pairs are reciprocally partially concatenated on the paternal haplotype to form a chimeric sequence. The maternal haplotype carries the wild-type. Upstream and downstream genomic regions are denoted by 'u' and 'd', respectively. **(B)** The copy number of gene pairs' genomic region on the paternal haplotype is increased, and the maternal haplotype is kept at one copy.

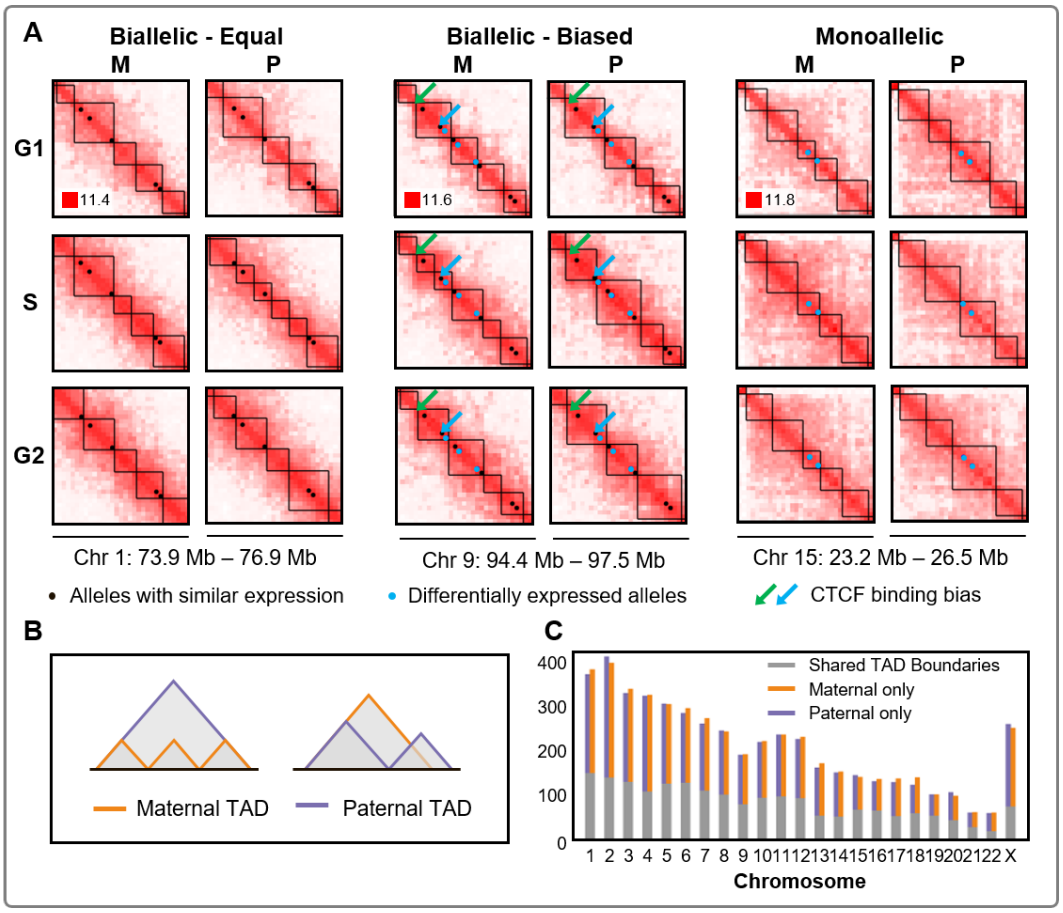

Fig. S6: Allele-specific topologically associated domains (TADs), related to **STAR Methods**. (**A**) Subsection of Chromosomes 1 (left), 9 (middle), and 15 (right) separated into allele- and cell cycle-specific matrices shown in log_2 scale 100 kb resolution, with TADs depicted as solid black lines. Circles in each setting represent allele-specific genes with similar (black) and differential (blue) expression. Arrows indicate a binding bias of CTCF to the maternal (green) or paternal (blue) genome (*7*). The CTCF binding data is not cell cycle separated. Arrows were added to all cell cycle phases, but CTCF binding may only be active at particular phases. TAD boundaries are found using the spectral identification method (*38*). **(B)** Schematic representation of allele-specific TADs. A single TAD in one genome can be identified as a multiple TADs in the other genome (left), or TAD boundaries can shift depending on local genome structure (right). **(C)** Bar graph highlighting the number of TAD boundaries in common between maternal and paternal (gray), maternal only TAD boundaries (orange), and paternal only TAD boundaries (purple) for all chromosomes in G1.

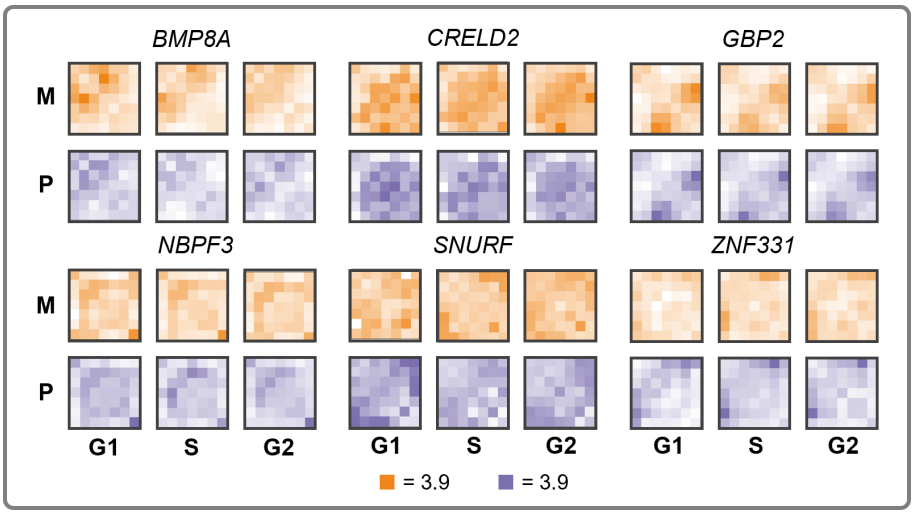

Fig. S7: Local Hi-C contact maps six example genes, related to **Figure 5B**. Legend at the bottom represents the maximum values of local Hi-C contacts for these genes. Orange and purple correspond to maternal and paternal local Hi-C contacts, respectively. Within this figure, G2 includes both G2 and M phase.

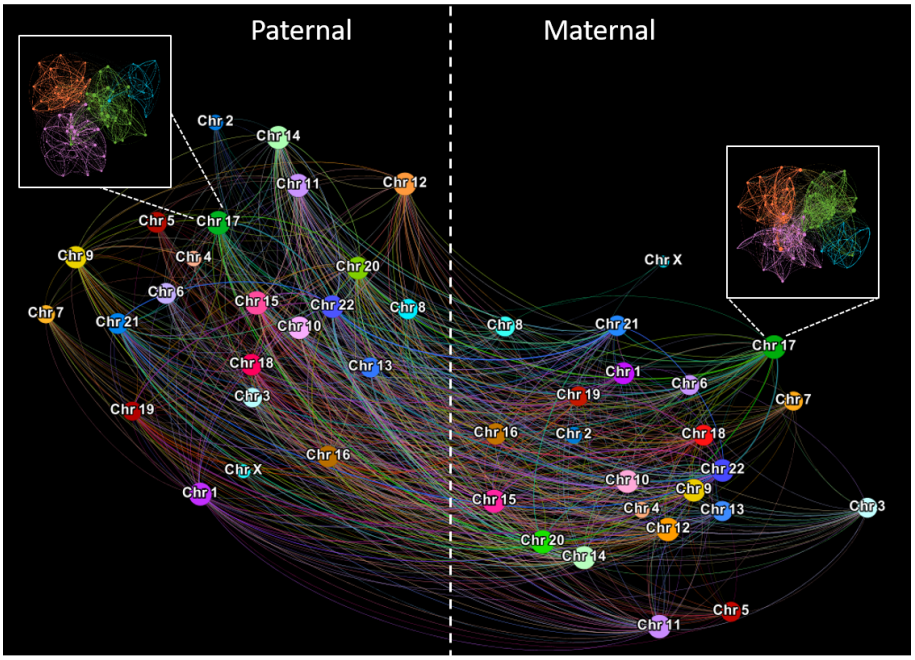

Fig. S8: Maternal and paternal genomes as a network of chromosomes, related to **STAR Methods**. The maternal and paternal chromosomes are separated to highlight inter-haplotype interactions from Hi-C data. Each chromosome has an internal network of intra-chromosomal chromatin contacts as highlighted in the maternal and paternal Chromosome 17.

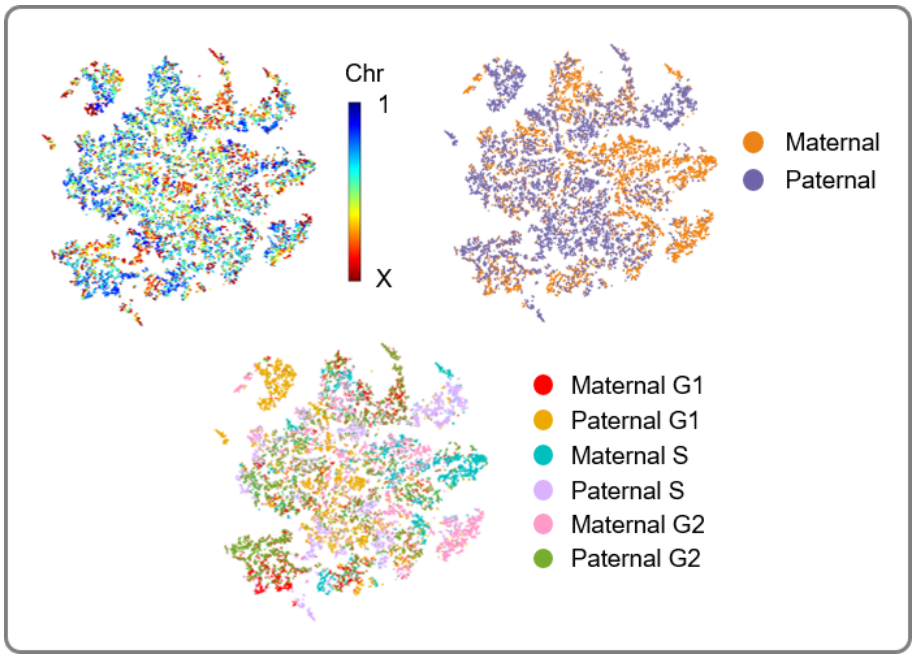

Fig. S9: Genome-wide visualization of the maternal and paternal 4DN, related to **STAR Methods**. Low dimensional representation (t-SNE) of structure and function for the maternal and paternal genomes across cell cycle phases in 1 Mb resolution (**Method Details**) (*77*). The three plots show the same data with different color schemes to highlight the locations of chromosomes (top left), parental origin (top right), and parental origin with cell cycle phase (bottom). Differences in the low dimensional mappings can be seen genome-wide for the maternal and paternal genomes, as well as cell cycle phases.

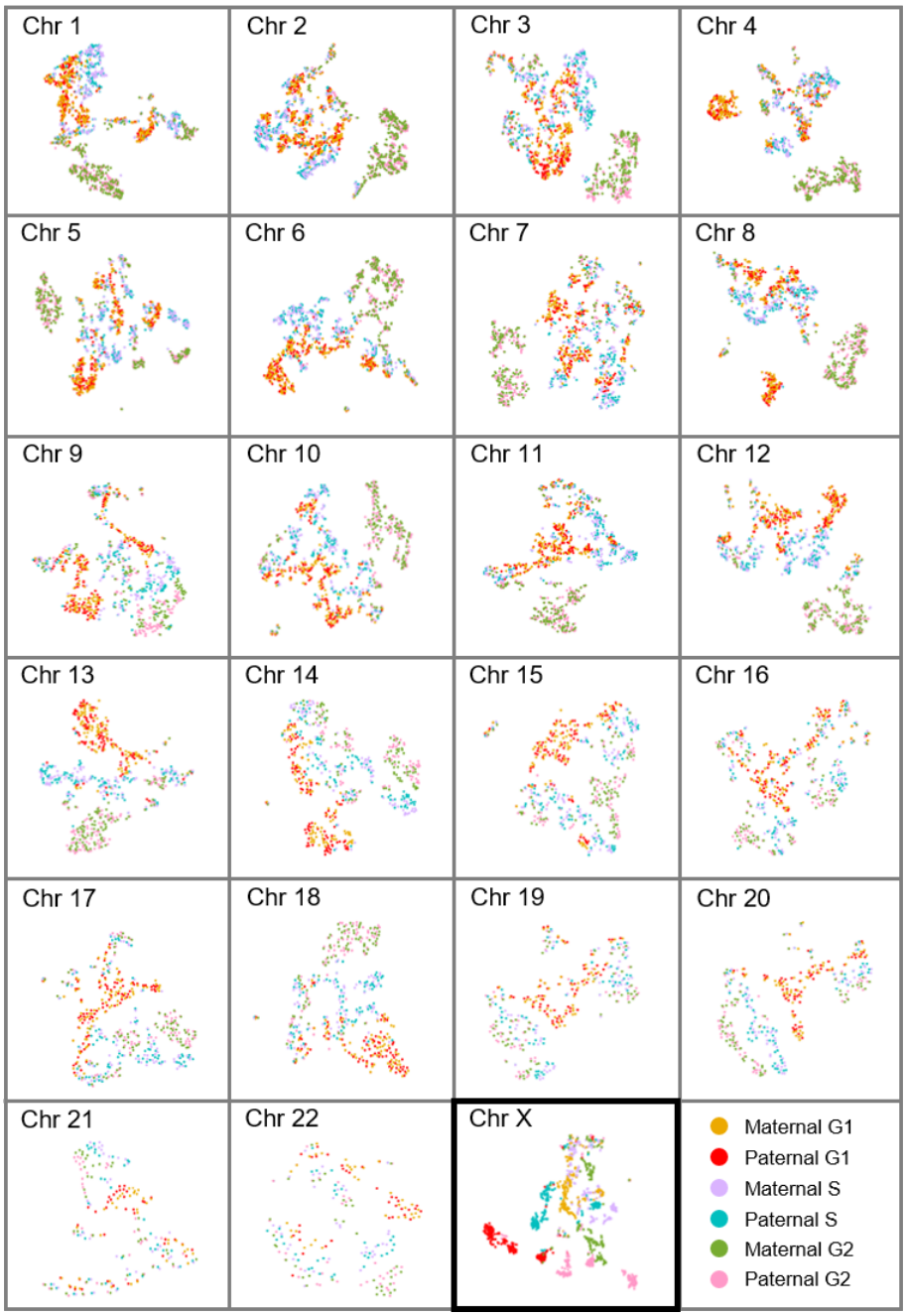

Fig. S10: The same process from **Figure S9** was applied to individual chromosomes, with color scheme highlighting parental origin and cell cycle phase, related to **STAR Methods**. The X Chromosome shows clear separation of the maternal and paternal copies. The autosomes have more subtle differences between their maternal and paternal low dimensional projections.

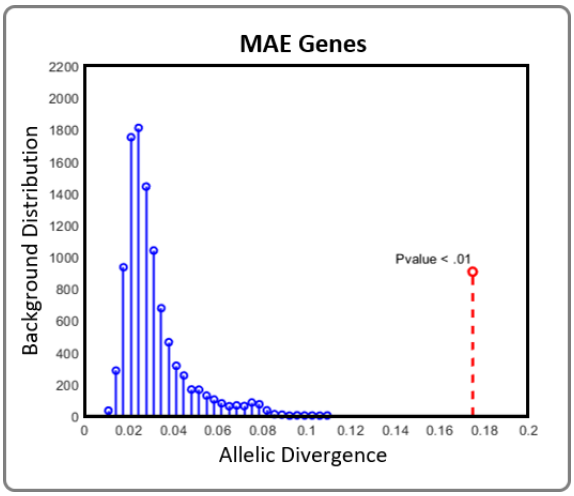

Fig. S11: Statistical significance of allelic divergence in monoallelicly expressed genes, related to **STAR Methods**. A permutation test was performed for a subset of monoallelicly expressed genes to determine whether their allelic divergence was significantly higher than randomly sampled allele-specific genes (**Method Details**).